179 180	Supplementary figure legends
181	Fig. E1. mRNA and protein expression of mutant IKAROS. (A) Relative quantification of
182	IKZF1 mRNA in B cells from healthy controls (C1-C3) and patients (P1, P2) normalized to the
183	average of the three housekeeping genes (GAPDH, Actin, HPRT) and relative to C1 (two
184	repeats in triplicate). (B) Representative western blot analysis of IKAROS expression in
185	whole protein lysates from EBV-transformed B cells from P1, P2, C4 and C5. (C)
186	Quantification of IKAROS protein from western blot in B, normalized to histone H1 (4
187	technical replicates).
188	
189	Fig. E2 Representative EMSAs using FLAG-tagged expression plasmids. (A)
190	Representative western blot of nuclear enriched fractions from HEK293T cells transfected
191	with Flag-tagged plasmids containing 100% WT IKAROS, 100% L188V mutant IKAROS,
192	WT:L188V IKAROS in a 50:50 ratio or 100% p.173-253del control (two repeats). (B) Western
193	blot of the nuclear extracts in (A) using anti-Flag antibodies as in A but normalized to WT
194	expression for use in EMSA (two repeats). (C) EMSAs were performed using two different
195	probes: IK-bs4 and YSat8 as indicated. Lanes were loaded with nuclear extracts from
196	untransfected HEK cells (Untr) or HEK cells transfected with 100% WT, 100% mutant L188V,
197	WT:L188V in a 50:50 ratio or 100% p.173-253del control. A supershift was induced by adding
198	anti-Flag antibody. (D) Lanes were loaded with nuclear extracts containing the same amount
199	of WT IKAROS but increasing amount of mutant L188V, supplemented with empty vector
200	(EV). The arrows mark the size of complexes containing IKAROS.
201	
202	Fig. E3. Representative EMSAs using HA-tagged WT and Flag-tagged L188V
203	expression plasmids. (A) Representative western blot of nuclear enriched fractions from
204	HEK293T cells transfected with HA-tagged WT driven by SV40 promoter and Flag-tagged
205	L188V mutant IKAROS driven by CAG promoter (three repeats to achieve normalization to
206	housekeeping genes). (B) Lanes were loaded with nuclear extracts containing the same
207	amount of HA-tagged WT IKAROS driven by the SV40 promotor and increasing amounts of

- 208 Flag-tagged L188V mutant IKAROS driven by the CAG promoter. Relative quantification for
- 209 each probe is shown on the far right (five independent experiments for IK-bs4, two for YSat8).

210 The arrows mark the size of complexes containing IKAROS.

211

212 Fig. E4. Mutant IKAROS feeds a pro-germinal center immunological phenotype. PBMCs were isolated from P1, P2 (together referred to as 'P' for patients), mother, brother and 3 213 214 healthy young adult controls (HC) to stain for a comprehensive B- and T cell panel (samples 215 from two different time points denoted by circles or triangles). P1 and P2 are always indicated 216 in blue and in red respectively. Error bars denote the standard error of the mean. (A) Total B 217 cell numbers as a percentage of total lymphocytes for P1 and P2 compared to HC. (B) TREC 218 and kappa-deleting recombination excision circles values. Pediatric controls (<18 yr) are 219 indicated by triangles and adult controls by circles. (C-G) B cell subsets of HC and P as a 220 percentage of CD19+ cells. (H) CD4+ and CD8+ T cells as a percentage of total lymphocytes 221 in HC and P. (I) CD4/CD8 ratio. (J-K) Naïve T cells and CD45RA+ effector memory T cells 222 (TEMRA) as a percentage of single positive CD8+ T cells in age-matched HC and P2. (L-M) 223 Regulatory T cells (Treg) and follicular helper T cells (Tfh) as a percentage of single positive 224 CD4+ cells in HC and P. (N) Follicular regulatory T cells (Tfr) in HC and P as a percentage of 225 CD25+Foxp3+ Treg.

226

Fig. E5. Decreased naïve antigen receptor repertoire diversity in patients with L188V

228 **IKAROS.** (A) V gene and (B) J gene usage in purified B cells from 10 healthy controls (grey) 229 as well as P1 (blue) and P2 (red). (C) Junction characteristics of mutant IKAROS patients 230 compared to 10 healthy controls (HC). Median number of total deletions, N-nucleotide 231 additions and the CDR3 length of IGH rearrangements. (D) Diversity index of the naive B cell 232 repertoire in mutant IKAROS patients and age-matched HC. (E) The subclass distribution of 233 IGG and IGA transcripts with 7 age-matched controls for P1 and 6 age-matched controls for 234 P2. (F) Median percentage of somatic hypermutation (SHM) is shown for P1 and P2 and age-235 matched controls. Mean±SEM. Experiments in (A-F) were performed once.

236

Fig. E6. Proliferative potential of mutant IKAROS B cells using a CFSE assay. CFSE-

238 labeled B cells were negatively selected from P1, P2, mother, brother and 3 healthy controls

239 (HC), and stimulated in culture for 5 days with 10µg/ml anti-IgM mix + 1µg/ml anti-CD40L +

- 240 1µg/ml CpG (two repeats). (A) Representative plots gated for percentage of proliferating cells
- for both patients and 2 out of 5 controls. (B) Percentage of proliferating B cells from HC
- 242 versus P. (C) Proliferation index of HC versus P. (D) PBMCs stimulated with anti-IgM-IgA-IgG
- 243 10µg/ml or anti-IgM-IgA-IgG 10µg/ml + CD40L 1µg/ml for 24hrs were stained for Ki67.
- 244 Percentage of Ki67+ cells in the CD19+ population (two repeats).
- 245

247

246 Fig. E7. Hyperresponsive patient EBV transformed B cells. (A) Total Erk1/2 MFI on EBV

transformed B cells from P2 and unrelated HC (one repeat). (B) EBV transformed B cells

- stimulated with 10µg/ml anti-IgM-IgA-IgG were stained for pErk. Shaded area marks one
- standard deviation above and below the mean of the HC (Representative of two repeats). (C)
- 250 Baseline MFI of pErk on EBV transformed B cells from P2 and unrelated HC normalized to
- average of HC (two repeats).
- 252
- 253 Fig. E8. IKAROS binding to the CD22 locus. (A) Signal tracks of IKAROS ChIP-seq data
- from human GM12878 B-lymphocytes and human pre-B ALL. Location of the CD22 EMSA
- probes are indicated. (B) Representative CD22 EMSAs performed using two different probes:
- 256 CD22.1 and CD22.2 as indicated. Lanes were loaded with nuclear extracts from
- 257 untransfected HEK cells (Untr) or HEK cells transfected with 100% WT, 100% mutant L188V,
- 258 WT:L188V in a 50:50 ratio or 100% p.173-253del control. The arrows mark the size of
- 259 complexes containing IKAROS. A supershift was induced by adding anti-Flag antibody (three
- repeats). (C) ChIP-qPCR using IgG input from EBV transformed B cells of P2, HC and
- 261 GM12878 human B lymphocytes (three repeats).
- 262
- 263
- 264

265 Supplementary tables

266 Table E1. Laboratory values of P1 and of P2 at age 12 years

Parameter	P1 (Age 49y)	P2 (Age 12y)		
		Before treatment	After treatment*	
Lymphocytes (count/µL)	2300 (1200-3600)	2000 (1500–2000)	1600 (1000-5300)	
CD19 ⁺ (% of total lymphocytes)	16.8 (5.0 -20.0)	6.9 (8.0-24.0)	5.0 (8.0-24.0)	
CD19 ⁺ (count/ μ L of lymphocytes)	381 (82-476)	138 (200-600)	81 (200-600)	
CD3 ⁺ (% of total lympohocytes)	70.0 (58.0-84.0)	86.6 (52.0-78.0)	82.7 (52.0-78.0)	
CD3 ⁺ (count/µL of lymphocytes)	1594 (798-2823)	1733 (800-3500)	1340 (800-3500)	
Lupus anticoagulant Ab	Positive	Very strongly positive	Very strongly positive	
Anticardiolipin Ab (GPL/ml)	4 (≤20)	NA	NA	
Anticardiolipin IgG	NA	9.4 (≤2.5)	4.8 (≤2.5)	
Anticardiolipin IgM	NA	6.4 (≤3.5)	2.1 (≤3.5)	
	NA	Negative	Negative	
ANA**	Positive: nuclear,	Positive: nuclear,	Positive: nuclear,	
	fine speckled 1/160	homogeneous 1/1280	homogeneous 1/1280	
Anti-dsDNA Ab by Farr (IU/ml)	≤7	40.5	23.5	
IgG (g/L)	8.85 (7.51-15.60)	9.38 (5.76-12.65)	2.94 (5.76-12.65)	
IgA (g/L)	1.12 (0.82-4.53)	0.60 (0.81-2.32)	0.17 (0.81-2.32)	
IgM (g/L)	0.42 (0.46-3.04)	0.90 (0.30-1.59)	0.69 (0.30-1.59)	
Antibody response				
Pneumococcal polysaccharide	1	Normal	/	
Hepatitis B surface Ab (mIU/mI)	1	0.0 (≥10.0)	/	
Mumps IgG	1	Negative	/	
Measles IgG (mIU/ml)	1	430 (≥10.0)	/	
Rubellavirus IgG (IU/ml)		6.3 (≥10.0)	1	

267 * Current treatment four months after initiation comprised of 4mg corticosteroids, hydroxychloroquine, oral

268 anticoagulation and prophylactic amoxicilline.

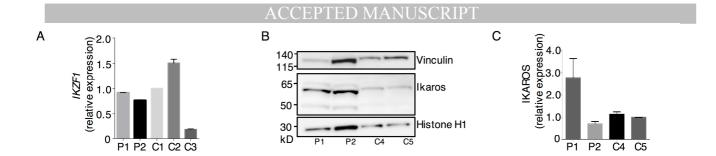
269 ** Other autoantibodies tested in P2 were negative: Ro60, SSB/La, U1-RNP, RNP-70, Sm, ScI-70 sensitive, Jo-1, Ro52

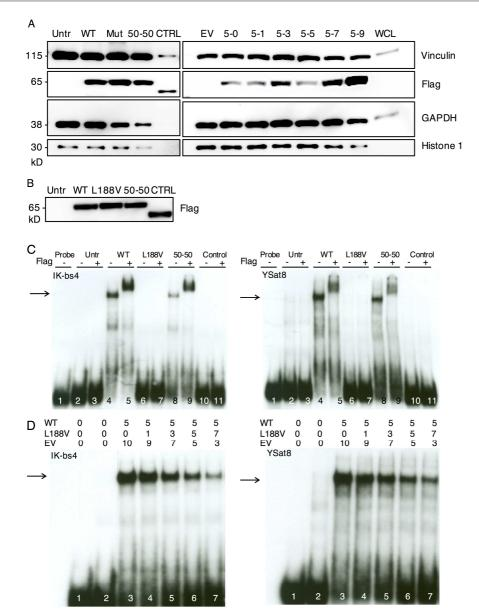
270

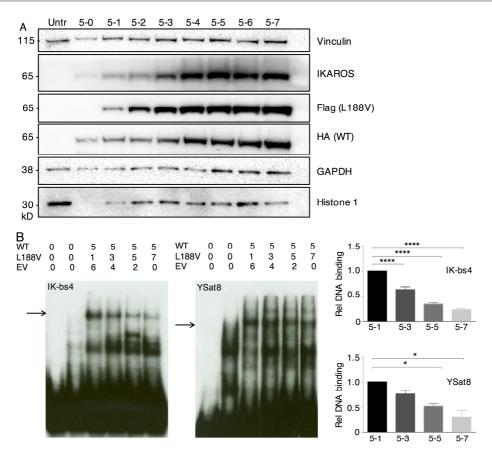
ANA = anti-nuclear antibodies, Ab = antibodies, anti-dsdNA = anti-double stranded DNA, IgG/IgA/IgM = immunoglobulin G/A/M

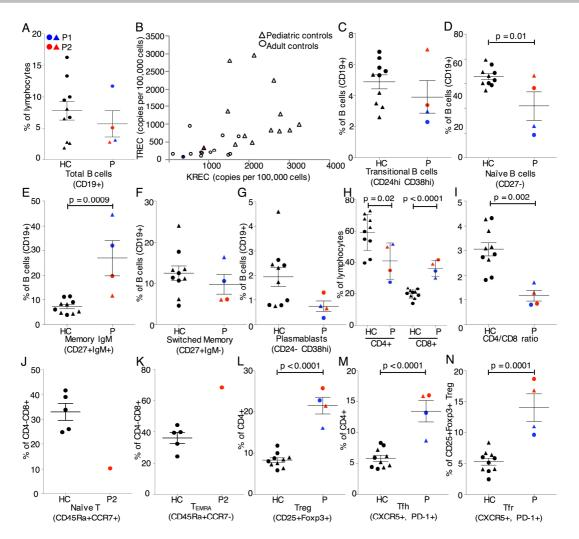
274	Supplementary references				
275	1.	Van Eyck L, De Somer L, Pombal D, Bornschein S, Frans G, Humblet-Baron S, et al.			
276		Brief report: IFIH1 mutation causes systemic lupus erythematosus with selective IgA			
277		deficiency. Arthritis Rheumatol. 2015;67(6):1592-1597.			
278	2.	Kircher M, Witten DM, Jain P, O'Roak BJ, Cooper GM, Shendure J. A general			
279		framework for estimating the relative pathogenicity of human genetic variants. Nat			
280		Publ Gr. 2014;46(3):310-315.			
281	3.	Itan Y, Shang L, Boisson B, Patin E, Bolze A, Moncada-Vélez et al. The human gene			
282		damage index as a gene-level approach to prioritizing exome variants. Proc Natl Acad			
283		Sci U S A. 2015;112(44):13615-13620.			
284	4.	Neitzel H. A routine method for the establishment of permanent growing			
285		lymphoblastoid cell lines. Hum Genet. 1986;Aug(73(4)):320-326.			
286	5.	Molnár A, Georgopoulos K. The Ikaros gene encodes a family of functionally diverse			
287		zinc finger DNA-binding proteins. Mol Cell Biol. 1994;14(12):8292-8303.			
288	6.	Sun L, Liu A, Georgopoulos K. Zinc finger-mediated protein interactions modulate			
289		Ikaros activity, a molecular control of lymphocyte development. EMBO J.			
290		1996;15(19):5358-5369.			
291	7.	van der Burg M, Kreyenberg H, Willasch A, Barendregt BH, Preuner S, Watzinger F,			
292		et al. Standardization of DNA isolation from low cell numbers for chimerism analysis			
293		by PCR of short tandem repeats. Leuk Off J Leuk Soc Am Leuk Res Fund, UK.			
294		2011;25(9):1467-1470.			
295	8.	Driessen GJ, Ijspeert H, Weemaes CMR, Haraldsson Á, Trip M, Warris A, et al.			
296		Antibody deficiency in patients with ataxia telangiectasia is caused by disturbed B-			
297		and T-cell homeostasis and reduced immune repertoire diversity. J Allergy Clin			
298		Immunol. 2013;131(5).			
299	9.	IJspeert H, Wentink M, van Zessen D, Driessen GJ, Dalm VA, van Hagen, MP, et al.			
300		Strategies for B-cell receptor repertoire analysis in primary immunodeficiencies: from			
301		severe combined immunodeficiency to common variable immunodeficiency. Front			
302		Immunol. 2015;6(April):157.			
303	10.	van Dongen JJ, Langerak AW, Brüggemann M, Evans PA, Hummel M, Lavender FL,			

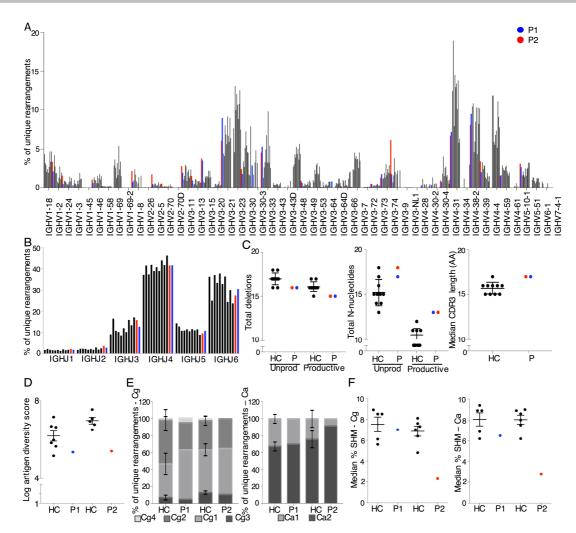
		ACCEPTED MANUSCRIPT
304		et al. Design and standardization of PCR primers and protocols for detection of clonal
305		immunoglobulin and T-cell receptor gene recombinations in suspect
306		lymphoproliferations: report of the BIOMED-2 Concerted Action BMH4-CT98-3936.
307		Leukemia. 2003;17(October):2257-2317.
308	11.	Moorhouse MJ, van Zessen D, IJspeert H, Hiltemann S, Horsman S, van der Spek PJ,
309		et al. ImmunoGlobulin galaxy (IGGalaxy) for simple determination and quantitation of
310		immunoglobulin heavy chain rearrangements from NGS. BMC Immunol.
311		2014;15(1):59.
312	12.	IJspeert H, van Schouwenburg PA, van Zessen D, Pico-Knijnenburg I, Stubbs AP, van
313		der Burg M. Antigen Receptor Galaxy: A User-Friendly, Web-Based Tool for Analysis
314		and Visualization of T and B Cell Receptor Repertoire Data. J Immunol. 2017.
315	13.	Alamyar E, Duroux P, Lefranc MP , Giudicelli V. IMGT($^{(\!R\!)}$) tools for the nucleotide
316		analysis of immunoglobulin (IG) and T cell receptor (TR) V-(D)-J repertoires,
317		polymorphisms, and IG mutations: IMGT/V-QUEST and IMGT/HighV-QUEST for
318		NGS. Methods Mol Biol. 2012;(882):569-604.
319	14.	IJspeert H, van Schouwenburg PA, van Zessen D, Pico-Knijnenburg I, Driessen GJ,
320		Stubbs AP, et al. Evaluation of the Antigen-Experienced B-Cell Receptor Repertoire in
321		Healthy Children and Adults. Front Immunol. 2016;7(October):410.
322	15.	Tiller T, Meffre E, Yurasov S, Tsuiji M, Nussenzweig MC, Wardemann H. Efficient
323		generation of monoclonal antibodies from single human B cells by single cell RT-PCR
324		and expression vector cloning. J Immunol Methods. 2008;329(1-2):112-124.
325	16.	Berkowska MA, Schickel JN, Grosserichter-Wagener C, de Ridder D, Ng YS, van
326		Dongen JJ, et al. Circulating Human CD27-IgA+ Memory B Cells Recognize Bacteria
327		with Polyreactive Igs. J Immunol. 2015;195(4):1417-1426.
328	17.	Schjerven H, Ayongaba EF, Aghajanirefah A, McLaughlin J, Cheng D, Geng H, et al.
329		Genetic analysis of Ikaros target genes and tumor suppressor function in BCR-ABL1+
330		pre–B ALL. 2017:1-22.
331	18.	Levy C, Fusil F, Amirache F, Costa C, Negre D. Baboon envelope pseudotyped
332		lentiviral vectors efficiently transduce human B cells and allow active factor IX B cell
333		secretion in vivo in NOD/SCIDγc-/- mice. 2016:2478-2492.

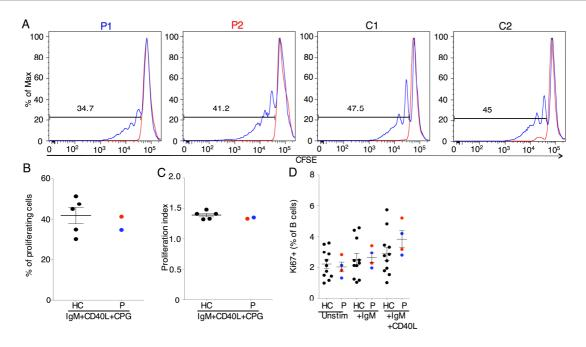




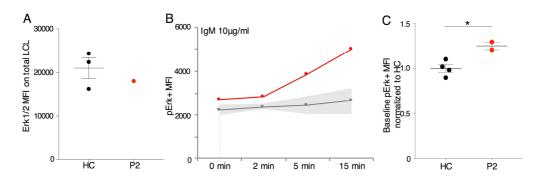


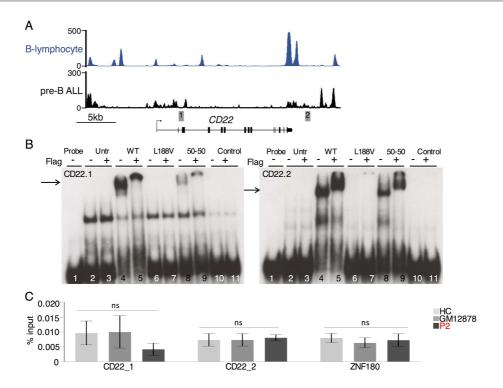






я. Х





37

C Y